# Size Effect on Flexural and Shear Behavior of PVA-ECC

Toshiyuki Kanakubo, Dr.E.
University of Tsukuba, Japan
Katsuyuki Shimizu, Dr.E.
Railway Technical Research Institute, Japan
Tetsushi Kanda, Dr.E.
Kajima Technical Research Institute, Japan

## Abstract

High Performance Fiber-Reinforced Cementitious Composites (HPFRCC), which show a strain hardening branch and multiple cracking under uniaxial tensile stress, have been focused by lots of researchers because of its unique mechanical performance. Engineered Cementitious Composites (ECC) exhibit a maximum tensile strain of several percent owing to the synergetic effect of high-performance fiber and specifically designed mortar matrix. Unprecedented high-performance structural members can be expected when ECC is applied to seismic components. It is considered that the fiber in fiber-reinforced cementitious composite causes scale effect which is mainly influenced by fiber orientation. For example, the small size of specimens such as plate type shows higher tensile strength and deformation capacity because of two-dimensional fiber orientation.

This paper describes the test results of bending and shear test of ECC which is reinforced by polyvinyl alcohol fiber (PVA-ECC). The adopted test methods are 4-point bending test and Ohno type shear test to obtain fundamental flexural and shear behaviors of PVA-ECC, respectively. The test parameters are sectional size of specimens and fiber volume fraction of PVA fiber. Test results are mainly discussed on flexural / shear strength and deformation capacity influenced by sectional size. The ratio of experimental strength to calculated one is evaluated by volume of specimens.

***Keywords***: Engineered Cementitious Composite, flexural strength, shear strength, bending test, shear test.

---

Toshiyuki Kanakubo
Dept. of Engineering Mechanics and Energy, University of Tsukuba
1-1-1, Tennhdai, Tsukuba-city, 305-8573
Japan

Email: kanakubo@kz.tsukuba.ac.jp
Tel: +81 29 853 5045

## 1.0 Introduction

High Performance Fiber-Reinforced Cementitious Composites (HPFRCC), which show a strain hardening branch and multiple cracking (Figure 1) under uniaxial tensile stress, have been focused by lots of researchers because of its unique mechanical performance. Engineered Cementitious Composites (ECC) exhibit a maximum tensile strain of several percent owing to the synergetic effect of high-performance fiber and specifically designed mortar matrix. Unprecedented high-performance structural members can be expected when ECC is applied to seismic components [1].

It has been cleared that cementitious materials such as concrete show scale effect on their mechanical properties due to size of aggregates, existence of air void, and so on. In addition, it is considered that the fiber in fiber-reinforced cementitious composite causes scale effect which is mainly influenced by fiber orientation. For example, the small size of specimens such as plate type shows higher tensile strength and deformation capacity because of two-dimensional fiber orientation [2]. If we use some test pieces to check the mechanical properties of HPFRCC, it is necessary to have information about the relationships between properties obtained by test pieces and those in actual structures.

This paper describes the test results of bending and shear test of ECC which is reinforced by polyvinyl alcohol fiber (PVA-ECC). The adopted test methods are 4-point bending test and Ohno type shear test to obtain fundamental flexural and shear behaviors of PVA-ECC, respectively. The test parameters are sectional size of specimens and fiber volume fraction of PVA fiber. Test results are mainly discussed on flexural / shear strength and deformation capacity influenced by sectional size. The ratio of experimental strength to calculated one is evaluated by volume of specimens.

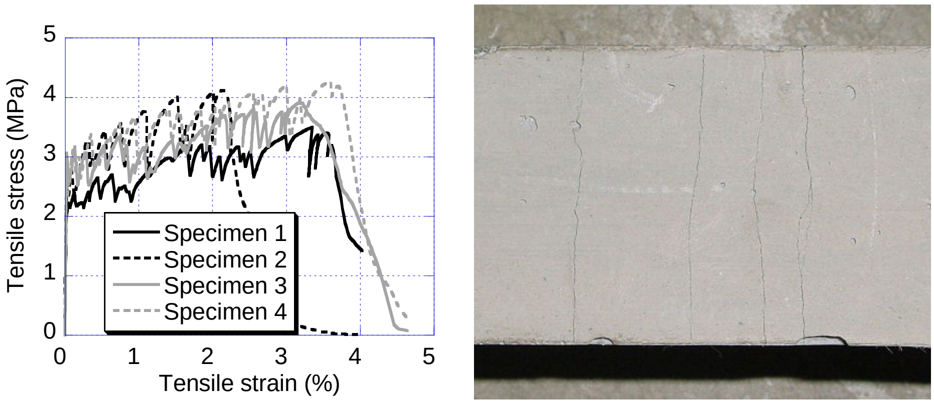

Figure 1. Strain hardening behavior and multiple cracking of ECC.

## 2.0 Outline of Loading Test

### 2.1 Specimen

The dimensions and reinforcing bar arrangements of the specimens are shown in Figure 2 and 3 for bending test and shear test, respectively. The lists of specimens are shown in Table 1 and 2.

Main parameters of bending test specimen are height of section (40mm, 100mm and 280mm) and presence of main bars. All specimens have same ratio of loading span to section height, and main bar ratio ($p_t$) is also same. 4-point loading is carried out using the universal loading machine. Measurement items are load and axial deformation between pure bending region along the upper and lower position as shown in Figure 2. The axial deformation is used for calculation of average curvature.

Main parameters of shear test specimen are height of section (50mm, 100mm and 280mm) and stirrup ratio ($p_w$). The ratio of shear span to section height is same as 1.25 for all specimens. Loading was carried out by Ohno method under anti-symmentrical moment with monotoric manner. LVDTs are set to measure relative displacement between the stubs.

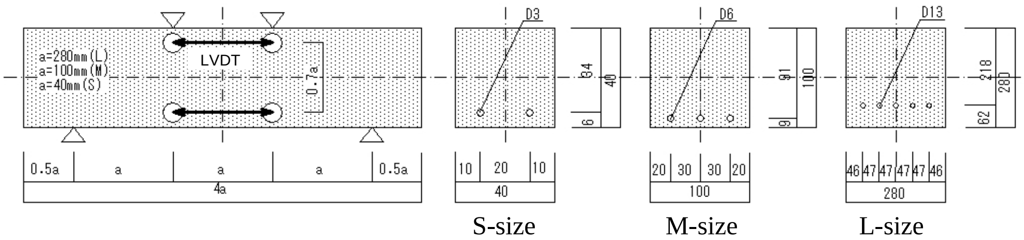


Figure 2. Bending test specimen.

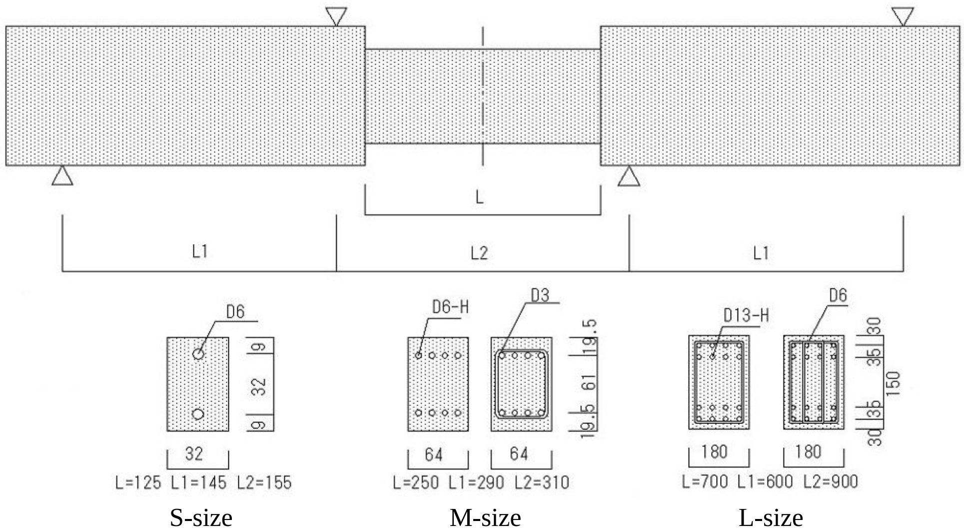


Figure 3. Shear test specimen.

**2.2 Material Properties of PVA-ECC**

PVA fiber shown in Table 3 was utilized in this research. Fiber volume fraction was set to 1.0, 1.5 and 2%. Water / binder ratio was 42.7%. Compressive strength at the testing age ranges from 40.3 to 44.4MPa by using 100 -200mm cylinder test piece. Hereafter, PVA-ECC with 1.0%, 1.5% and 2.0% volume fraction is identified as PVA10, PVA15 and PVA20, respectively.

Table 1. List of bending test specimen.

| Specimen | Fiber volume fraction $V_f$ (%) | Sectional size $b \times D$ (mm) | Main bar | |
|---|---|---|---|---|
| | | | Arrangement | Yeild strength (MPa) |
| PVA10-F-S | 1.0 | 40×40 | - | - |
| PVA15-F-S | 1.5 | | | |
| PVA20-F-S | 2.0 | | | |
| PVA10-FR-S | 1.0 | | 2-D3 $p_t$=1.04% | 222 |
| PVA15-FR-S | 1.5 | | | |
| PVA20-FR-S | 2.0 | | | |
| PVA10-F-M | 1.0 | 100×100 | - | - |
| PVA15-F-M | 1.5 | | | |
| PVA20-F-M | 2.0 | | | |
| PVA10-FR-M | 1.0 | | 3-D6 $p_t$=1.04% | 382 |
| PVA15-FR-M | 1.5 | | | |
| PVA20-FR-M | 2.0 | | | |
| PVA10-F-L | 1.0 | 280×280 | - | - |
| PVA15-F-L | 1.5 | | | |
| PVA20-F-L | 2.0 | | | |
| PVA10-FR-L | 1.0 | | 5-D13 $p_t$=1.04% | 363 |
| PVA15-FR-L | 1.5 | | | |
| PVA20-FR-L | 2.0 | | | |

Table 2. List of shear test specimen.

| Specimen | Fiber volume fraction $V_f$ (%) | Section $b \times D$ (mm) | Main bar | | Stirrup | | |
|---|---|---|---|---|---|---|---|
| | | | Arrangement | Yld. (MPa) | Arrangement | Yld. (MPa) | $p_w$ (%) |
| PVA10-00-S | 1.0 | 32×50 | 1-D6 $p_t$ =2.41% | 729 | - | - | 0.00 |
| PVA10-00-M | | 64×100 | 4-D6 $p_t$ =2.43% | 729 | | | |
| PVA10-89-M | | | | | 2-D3@25 | 222 | 0.89 |
| PVA10-89-L | | 180×280 | 8-D13 $p_t$ =2.43% | 722 | 2-D6@40 | 382 | 0.89 |
| PVA10-120-L | | | | | 4-D6@59 | 382 | 1.20 |
| PVA15-00-S | 1.5 | 32×50 | 1-D6 $p_t$ =2.41% | 729 | - | - | 0.00 |
| PVA15-00-M | | 64×100 | 4-D6 $p_t$ =2.43% | 729 | | | |
| PVA15-89-M | | | | | 2-D3@25 | 222 | 0.89 |
| PVA15-89-L | | 180×280 | 8-D13 $p_t$=2.43% | 722 | 2-D6@40 | 382 | 0.89 |
| PVA15-120-L | | | | | 4-D6@59 | 382 | 1.20 |
| PVA20-00-S | 2.0 | 32×50 | 1-D6 $p_t$ =2.41% | 729 | - | - | 0.00 |
| PVA20-00-M | | 64×100 | 4-D6 $p_t$ =2.43% | 729 | | | |
| PVA20-89-M | | | | | 2-D3@25 | 222 | 0.89 |
| PVA20-89-L | | 180×280 | 8-D13 $p_t$ =2.43% | 722 | 2-D6@40 | 382 | 0.89 |
| PVA20-120-L | | | | | 4-D6@59 | 382 | 1.20 |

Lots of uniaxial tension test methods for cementitious composites have been proposed and investigated by the numbers of researchers. In actual fact, however, uniaxial tension test requires special loading equipment, mold and much time to perform. In this research, the bending test which is specified as Japan Concrete Institute Standard (JCI-S-003-2005) [3] is adopted (Figure 4). Evaluation method for tensile strength and ultimate tensile strain of fiber reinforced cementitious composites has been introduced as the Appendix of JCI-S-003-2005. The evaluation method is introduced based on the following assumptions for stress distribution under the maximum bending moment as shown in Figure 4.

i) The stress distribution on the compression side is triangular.

ii) The stress distribution on the tension side is uniform ($f_{t,b}$).

These assumptions represent a state in which the strain on the tension edge has reached the ultimate strain ($\varepsilon_{tu,b}$) but the stress on the compression edge has not reached the compressive strength under the maximum bending moment. It is considered that these assumptions generally agree with actual strain and stress distributions of ECC. Table 4 summarized compression test and bending test results. Bending test results are obtained by the specimens PVA10-F-M, PVA15-F-M and PVA20-F-M.

Table 3. Mechanical properties of PVA fiber.

| Fiber length (mm) | Fiber diameter (mm) | Tensile strength (MPa) | Elastic modulus (GPa) |
|---|---|---|---|
| 12 | 0.040 | 1600 | 40 |

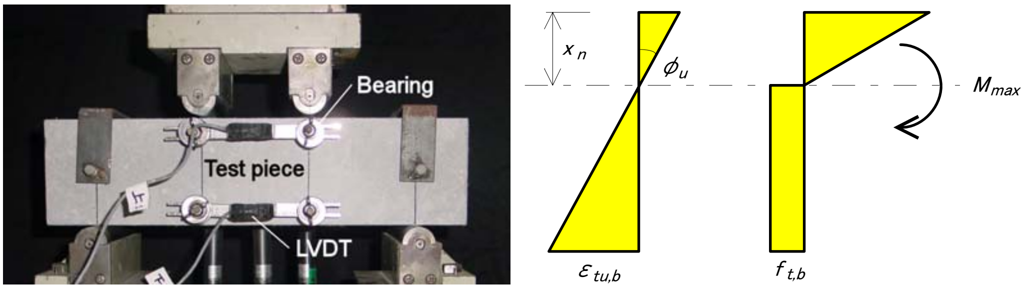


Strain distribution Stress distribution

Figure 4. Bending test setup and evaluation method by JCI-S-003-2005.

Table 4. Mechanical properties of PVA-ECC.

| ID | Compression | | | Tension | |
|---|---|---|---|---|---|
| | Elastic modulus (GPa) | Compressive strength (MPa) | Strain at max. (%) | Tensile strength (MPa) | Ultimate strain (%) |
| PVA20 | 16.7 | 42.5 | 0.53 | 4.76 | 1.07 |
| PVA15 | 17.4 | 42.0 | 0.42 | 2.39 | 0.42 |
| PVA10 | 18.1 | 40.2 | 0.40 | 2.83 | 0.58 |

## 3.0 Test Results

### 3.1 Bending Test

Examples of crack patterns after loading are shown in Figure 5 and 6. As shown in Figure 5, in the specimens without main bars, cracks took place over the pure bending region uniformly in S-size specimens, while multiple cracks concentrated in the certain region in M and L-size specimens. While the number of cracks is larger in L-size specimens, crack spacing is smaller in S-size specimens. As shown in Figure 6, in the specimens with main bars, fine cracks took place uniformly with the crack spacing as almost 4mm.

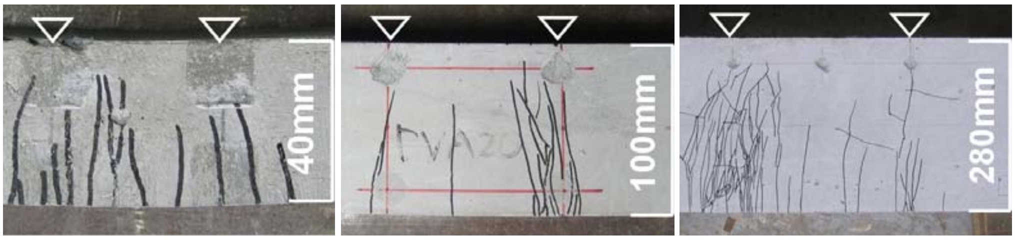


PVA20-F-S PVA20-F-M PVA20-F-L

Figure 5. Crack patterns of bending test specimen without main bars after loading.

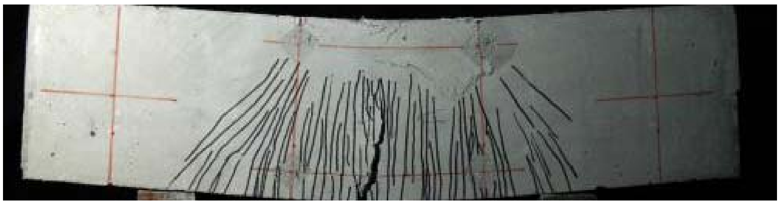

PVA20-FR-M

Figure 6. Crack patterns of bending test specimen with main bars after loading.

Relationships between bending stress and bending strain are shown in Figure 7. Bending stress is calculated by bending moment divided by modulus of section. Bending strain is defined as curvature at pure bending region multiplied by half of section height. Deflection hardening behavior which means that load increases after first cracking is observed in all the specimens. In the specimens with main bars, maximum bending stress is obtained by the compressive failure at the compression side. The maximum bending stress and deformation capacity of the specimen of PVA20 is larger than those of specimens of PVA15 and PVA10. The differences in bending stress and bending strain between L, M and S-size specimens without main bars are recognized remarkably. It is assumed that theses differences are due to fiber orientation that fiber direction

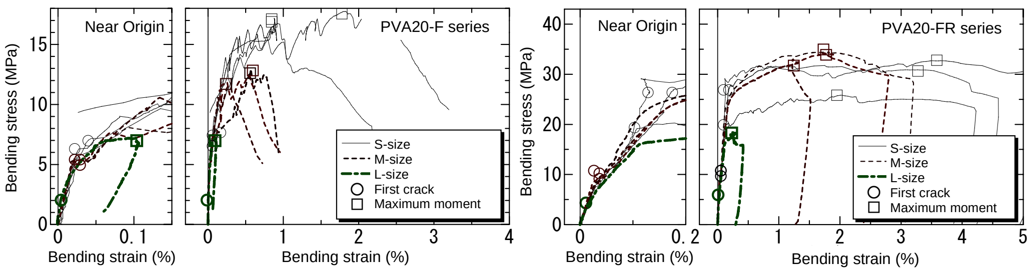


Figure 7. Bending stress - bending strain curve.

shows the tendency of placing along the axial direction in case of smaller specimens. In the specimens with main bars, maximum stress of M-size specimen shows higher value rather than S-size specimen. It is considered that this phenomenon is due to the difference of yield strength of main bars.

**3.2 Shear Test**

Examples of crack patterns after loading are shown in Figure 8. All specimens failed by shear with opening certain crack at the ultimate stage. Fine cracks were observed along the major crack. The difference of crack patterns by specimen size was not recognized. Relationships between shear stress and translational angle are shown in Figure 9. The shear stress is calculated from shear force divided by sectional area between tension and compression main bars. S-size specimens show higher shear strength rather than that of M-size specimen in case of no stirrup ($p_w$=0%). On the other hand, the shear strength of M-size specimen with stirrup ($p_w$=0.89%) is smaller than one of L-size specimen. The reason of this is considered that yield strength of stirrup of M-size specimen is smaller than that of L-size specimen.

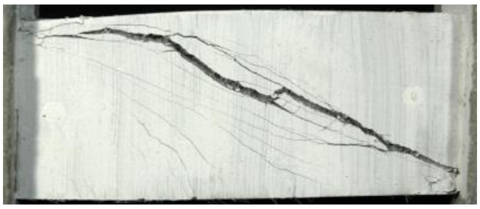
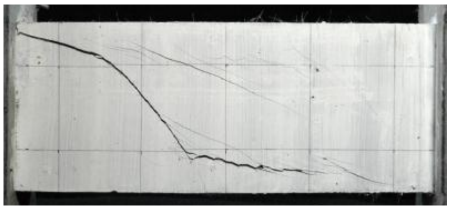

PVA20-00-S PVA20-00-M

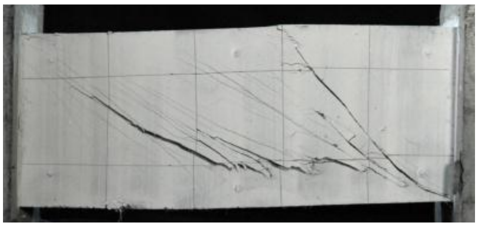
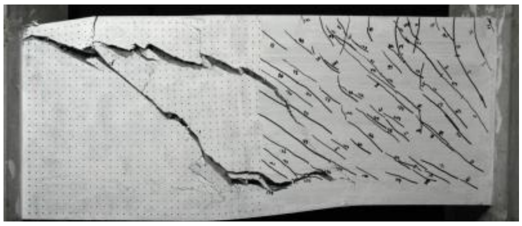

PVA20-89-M PVA20-89-L

Figure 8. Crack patterns of shear test specimen after loading.

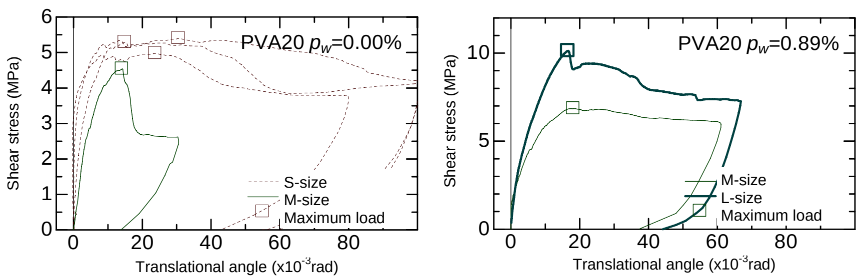


Figure 9. Shear stress - translational angle curve.

## 4.0 Evaluation of Flexural and Shear Strength

### 4.1 Flexural Strength

It has been reported that the flexural strength considering scale effect can be evaluated by high-stress volume of the specimen [4]. In this paper, tensile strength obtained by the method of the Appendix of JCI-S-003-2005 is evaluated using bending test specimens without main bars. The high-stress volume is assumed to be same as the volume of pure bending region. The relationship between high-stress volume ($V$) and tensile strength is shown in Figure 10. The tensile strength ($f_{t,b}$) is standardized by the tensile strength obtained by M-size specimen ($f_{t,b-M}$). In this figure, the test results of bending test specimen with steel fiber reinforced ultra high-strength concrete [5] are also indicated with the identification of DCT. The same tendency that small specimens show higher tensile strength can be recognized in spite of the differences of fiber volume fraction and fiber types. The following equation is obtained by regression analysis.

$$f_{t,b} / f_{t,b-M} = 6.72 \cdot V^{-0.144} \tag{1}$$

The tensile strength can be evaluated by Eq. (1) for any size specimen using tensile strength of M-size (section: 100x100mm) specimen. Using this relationship, flexural strength of the specimen with main bars is calculated by section analysis. The tensile stress – strain relationship of PVA-ECC is assumed to be perfect elastic-plastic model with the yield strength of $f_{t,b}$. Figure 11 shows the comparisons of flexural strength between experimental values and calculated ones. The average of the ratio of experimental values to calculated ones is 1.33.

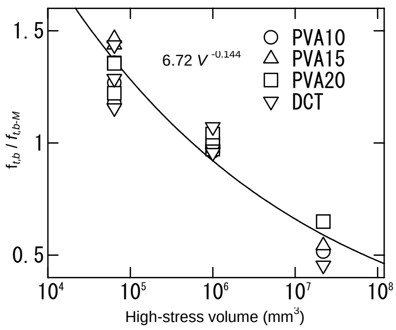


Figure 10. Relation between high-stress volume and tensile strength.

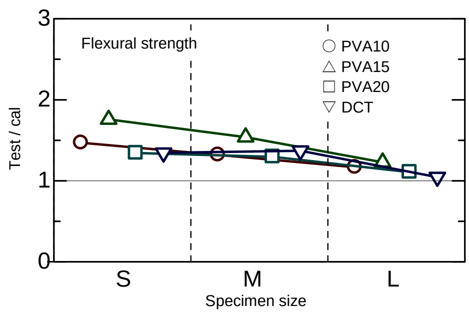


Figure 11. Comparison of flexural strength between experiment and calculation.

### 4.2 Shear Strength

The shear strength is evaluated by Japan Society of Civil Engineers (JSCE) Method [6] shown in the following equations. Tensile strength of PVA-ECC for each size of specimen is calculated using Eq. (1).

$$Q = Q_c + Q_s + Q_f \tag{2}$$

$Q_c$ : shear strength of member without stirrup (equal to ordinary RC member)

$$Q_c = \sqrt[4]{1/d} \cdot \sqrt[3]{100 p_t} \cdot \left(0.7 \times 0.20 \sqrt[3]{f_c}\right) \cdot b \cdot d$$

$Q_s$ : shear strength by stirrup (equal to ordinary RC member)

$$Q_s = p_w \cdot f_{wy} \cdot b \cdot (d / 1.15)$$

$Q_f$ : shear strength by HPFRCC (ECC)

$$Q_f = f_{t,b} \cdot b \cdot (d / 1.15)$$

where,

$d$ : effective height of member
$p_t$ : main bar ratio
$f_c$ : compressive strength
$p_w$ : stirrup ratio
$f_{wy}$ : yield strength of stirrup
$b$ : width of member
$f_{t,b}$ : tensile strength of HPFRCC (ECC)

Figure 12 shows the comparisons of shear strength between experimental values and calculated ones. The average of the ratio of experimental values to calculated ones is 1.28.

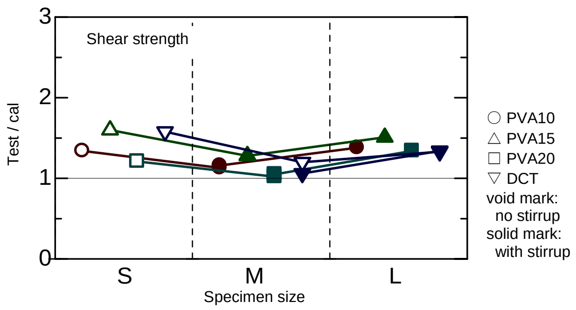


Figure 12. Comparison of shear strength between experiment and calculation.

## 5.0 Conclusions

This paper described the test results of bending and shear test of PVA-ECC. The test parameters were sectional size of specimens, presence of steel reinforcements and fiber volume fraction of PVA fiber. The size effect was observed that smaller specimen show higher strength and deformation capacity both for flexural and shear performance. Tensile strength of PVA-ECC was evaluated by 4-point bending test specified by JCI-S-003-2005 Method. Scale effect for the tensile strength was expressed by the high-stress volume of the specimen. The flexural strength and shear strength of the specimens show good agreements with calculated ones using evaluated tensile strength of PVA-ECC.

## 6.0 References


1. Kanda, T., Tomoe, S., Nagai, S., Maruta, M., Kanakubo, T. and Shimizu, K., “Full Scale Processing Investigation for ECC Pre-cast Structural Element,” *Journal of Asian Architecture and Building Engineering, Vol.5, No.2*, Architectural Institute of Japan, 2006, pp.333-340.
2. Kanakubo, T., “Tensile Characteristics Evaluation Method for Ductile Fiber-Reinforced Cementitious Composites,” *Journal of Advanced Concrete Technology, Vol.4, No.1*, Japan Concrete Institute, 2006, pp.3-17.
3. Japan Concrete Institute, “Method of test for bending moment – curvature curve of fiber-reinforced cementitious composites (JCI-S-003-2005),” *Journal of Advanced Concrete Technology, Vol.4, No.1*, Japan Concrete Institute, 2006, pp.73-78.
4. Urano, T., Murakami, K., Mitsui, Y. and Shigaki, T., “Studies on Application to Flexural Analysis of Tension-Softening and Its Size Effect of Steel Fiber Reinforced Concrete,” *Journal of Structural and Construction Engineering, No.463*, Architectural Institute of Japan, 1994, pp.1-7 (in Japanese).
5. Shimizu, K., Kudoh, S. and Kanakubo, T., “Size Effect on Flexural and Shear Behavior of DFRCC,” *Proceedings of the Japan Concrete Institute, Vol.28*, Japan Concrete Institute, 2007 (in Japanese).
6. Japan Society of Civil Engineers, “Recommendations for Design and Construction of High Performance Fiber Reinforced Cement Composite with Multiple Fine Cracks,” *Concrete Library 127*, Japan Society of Civil Engineers, 2007, pp.30-31.